

RESEARCH

Open Access



# DNMT3B promotes the progression of pheochromocytoma by mediating the hypermethylation of *LRP1B* promoter

Min Sun<sup>1</sup>, Yanrong Ma<sup>2</sup>, Jing Wan<sup>3</sup>, Bingli Zheng<sup>4</sup>, Zhenfeng Shi<sup>1\*</sup> and Jiuzhi Li<sup>1\*</sup>

## Abstract

**Background** Pheochromocytoma (Pheo) represents a potential metastatic neuroendocrine tumor. As a tumor suppressor gene, *LRP1B* is involved in the regulation of tumor progression. However, the precise regulatory mechanism of *LRP1B* in Pheo remains elusive.

**Methods** RT-QPCR, western blot and immunohistochemistry (IHC) were used to identify the expression levels of *DNMT3B* and *LRP1B*. Biochemistry assays including luciferase and ChIP were utilized to detect the interaction between the methyltransferase DNMT3B and *LRP1B* promoter. *LRP1B* or *DNMT3B* were knock-down in Pheo cell line by shRNAs. Functional experiments including clonal formation, migration, and in vivo transplantation were performed to evaluate the regulation of *LRP1B* or DNMT3B on tumor growth.

**Results** *LRP1B* was down-regulated, while *DNMT3B* was up-regulated in Pheo. Overexpression of *LRP1B* or inhibition of *DNMT3B* inhibited the progress of Pheo. DNMT3B was responsible for the hypermethylation of *LRP1B* promoter in Pheo. At the same time, overexpression of *DNMT3B* reversed the inhibitory effect of overexpression of *LRP1B* on Pheo progression.

**Conclusion** DNMT3B mediated the hypermethylation of the tumor suppressive gene *LRP1B* and promotes Pheo progression.

## Highlights

- *LRP1B* is down-regulated in pheochromocytoma.
- The promoter of *LRP1B* is hypermethylated in pheochromocytoma cells.
- *LRP1B* inhibits pheochromocytoma progression and metastasis.
- DNMT3B mediates the DNA methylation of *LRP1B* promoter in pheochromocytoma.

**Keywords** Pheochromocytoma, *LRP1B*, DNA methylation, DNMT3B

\*Correspondence:

Zhenfeng Shi  
shi\_zhengfeng@163.com  
Jiuzhi Li  
Lijiuzhi\_8@163.com

<sup>1</sup>Department of Urology Surgery Center, People's Hospital of Xinjiang Uygur Autonomous Region, No. 91, Tianchi Road, Tianshan District, Urumqi City, Xinjiang Uygur Autonomous Region 830000, China

<sup>2</sup>Department of Endocrinology and Metabolic Diseases, People's Hospital of Xinjiang Uygur Autonomous Region, Urumqi City, Xinjiang Uygur Autonomous Region, China

<sup>3</sup>Department of Ultrasound, People's Hospital of Xinjiang Uygur Autonomous Region, Urumqi City, Xinjiang Uygur Autonomous Region, China

<sup>4</sup>Department of Hepatobiliary Pancreatic Center, People's Hospital of Xinjiang Uygur Autonomous Region, Urumqi City, Xinjiang Uygur Autonomous Region, China



© The Author(s) 2025. **Open Access** This article is licensed under a Creative Commons Attribution-NonCommercial-NoDerivatives 4.0 International License, which permits any non-commercial use, sharing, distribution and reproduction in any medium or format, as long as you give appropriate credit to the original author(s) and the source, provide a link to the Creative Commons licence, and indicate if you modified the licensed material. You do not have permission under this licence to share adapted material derived from this article or parts of it. The images or other third party material in this article are included in the article's Creative Commons licence, unless indicated otherwise in a credit line to the material. If material is not included in the article's Creative Commons licence and your intended use is not permitted by statutory regulation or exceeds the permitted use, you will need to obtain permission directly from the copyright holder. To view a copy of this licence, visit <http://creativecommons.org/licenses/by-nc-nd/4.0/>.

## Introduction

Pheochromocytoma (Pheo) is a rare neuroendocrine tumor mainly developing in an adrenal gland [1]. While most subtypes of Pheo are benign, it has been shown that 2-26% of Pheo subtypes were highly metastasis [2]. The occurrence and development of Pheo are often related to gene mutation, including gene point mutation, gene fusion and, copy number change [2]. Pheo tumor cells secrete catecholamines, causing headache, hypertension, palpitation, and even shock and stroke [3]. At present, surgery and radiopharmaceuticals are the main treatments for Pheo [4]. Nevertheless, all of the above treatments show limitations in the prevention of Pheo metastasis. Therefore, developing a precision therapy for Pheo by understanding the molecular mechanisms driving tumor progression and metastasis is of considerable importance.

As a member of LDL receptor family, tumor suppressor gene *LRP1B* (low density lipoprotein receptor-associated protein 1B) is located on chromosome 2q, containing more than 500 kilobases and more than 90 exons [5], [6]. Many findings have indicated the regulatory role of *LRP1B* in tumor progression, especially tumor metastasis. For example, downregulation of *LRP1B* in colorectal cancer cells can inhibit cell growth, migration and metastasis [7]. *LRP1B* is significantly associated with poor prognosis in breast cancer, especially with lymph node metastasis [8]. Given that whether *LRP1B* is involved in the progression of Pheo remains unknown, in this study we first analyzed the expression level of *LRP1B* in Pheo based on The Cancer Genome Atlas (TCGA) database. In addition, we showed that two CpG islands in the promoter region of *LRP1B* in Pheo cells were highly methylated, which could be a regulatory mechanism underlying the reduced expression of *LRP1B* in Pheo. Indeed, previous studies have shown that the expression of *LRP1B* is modulated by epigenetic modifications [9]. Moreover, we reported that the DNA methyltransferases DNMT3B could be responsible for the hypermethylation of *LRP1B* promoter in Pheo.

Overall, we indicated that the hypermethylation of *LRP1B* promoter mediated by DNMT3B in Pheo cells potentially promoted tumor progression and metastasis.

## Materials and methods

### Collection of clinical samples

Pheochromocytoma tissue ( $n=34$ ) and its adjacent tissues were taken from patients who underwent surgical resection in the People's Hospital of Xinjiang Uygur Autonomous Region. All Pheo patients have no other medical history (including other tumors, immune-related diseases, diabetes, etc.), and they did not undergo radiotherapy or chemotherapy before surgical resection. The written informed consent of all patients was obtained in this study. The experiment was approved by the Ethics Committee of the Hospital (No. KY2023060156).

### Cell culture and transfection

The rat pheochromocytoma (PC12) were obtained from American Type Culture Collection (ATCC) that have high norepinephrine transporter expression [10]. The control group was mouse adrenal medulla cells purchased from Shanghai LMAI Bio (LM-011, Shanghai, China). PC12 and adrenal medulla cells were cultured in DMEM complete medium (Gibco, USA) containing 10% fetal bovine serum (FBS, Gibco) and 1% penicillin/streptomycin. The cells were placed in an incubator with 5% CO<sub>2</sub> at 37°C.

The *LRP1B* overexpression vector (oe-*LRP1B*-1, oe-*LRP1B*-2, and oe-*LRP1B*-3), shRNA containing *DNMT3B* target (sh-*DNMT3B*-1, sh-*DNMT3B*-2, and sh-*DNMT3B*-3), sh-DNMT1, sh-DNMT3A, and its negative control (NC) were all designed and synthesized by GenePharma (Shanghai, China). Lipofectamine 3000 (Thermo Fisher) was used for all cell transfections. ShRNAs sequences were listed in Table 1.

### Immunohistochemistry (IHC)

Clinical Pheo tissues or Pheo transplanted tumor mouse tissues were collected. The tissues were fixed with 10% formalin and then made into paraffin sections. After dewaxing and rehydration, 30% hydrogen peroxide was used to block the activity of oxidase. Next, the slices were incubated with normal goat serum to reduce nonspecific binding. The slices were incubated with primary antibody at 4°C overnight. Next, a biotin-coupled secondary antibody was used to treat with slices at room temperature for 2 h. After that, 3,3'-diaminobenzidine and hematoxylin were used to dye the slices for color reaction. Finally, the staining results were observed under an optical microscope (Olympus Corporation, Japan). The primary antibodies used were: anti-*LRP1B* (1:200, # PA5-115522, Thermo Fisher Scientific, MA, USA) and anti-Ki67 (1:200, ab15580, Abcam, Cambridge, UK). The staining was scored as the intensity of the positive staining (0 - negative, 1 - weak, 2 - moderate, 3 - strong) multiplied by the staining areas (0 = negative, 1 = 1–9%, 2 = 10–39%,

**Table 1** ShRNA sequence information

	sequence
sh- <i>DNMT3B</i> -1	CCCTACAGTGAGTCTTAATT
sh- <i>DNMT3B</i> -2	CCCUACAGUGAGUCCUUAAUU
sh- <i>DNMT3B</i> -3	UUGUUGUGACUAGCCUUAAUU
sh- <i>DNMT3A</i>	GGTGACTTCTGCAGCTAATAA
sh- <i>DNMT1</i>	GACCGATGCGGAGGCATTTAT

**Table 2** RT-qPCR primer sequence

Gene name	Species	Forward primer	Reverse primer
<i>DNMT1</i>	<i>Rattus norvegicus</i>	AGGACCCAGACAGAGAAGCA	GTACGGGAATGCTGAGTGGT
<i>DNMT3A</i>	<i>Rattus norvegicus</i>	CCAGATGTTCTTTGCCAATAA	GCAGACCAACATCGAATCCAT-
<i>DNMT3B</i>	<i>Rattus norvegicus</i>	ACAACCATTGACTTTGCCGC	CGTTCTCGGCTCTCCTCATC
<i>LRP1B</i>	<i>Rattus norvegicus</i>	TTTCTCCTCGCCTTACTCACT	CACACAACGTCTGATCTCGGT
<i>GAPDH</i>	<i>Rattus norvegicus</i>	AGTGCCAGCCTCGTCTCATA	GGTAACCGAGCGTCCGATAC
<i>LRP1B</i>	<i>Homo sapiens</i>	ATGTCCGAGTTTCTCCTCGC	TATCTGCAAGCATGCCCCAG
<i>GAPDH</i>	<i>Homo sapiens</i>	TCTGACTTCAACAGCGACAC C	AGCCAAATTCGTTGTCATACCA G

3 = 40–69%, and 4 = 70–100%). These scores were independently determined by two pathologists.

### Real-time fluorescence quantitative polymerase chain reaction (RT-qPCR)

The PC12 cells or tissues to be detected were collected. Total RNA was obtained from PC12 cells or tissues using TRIzol reagent (Invitrogen, USA). Subsequently, cDNA was synthesized by FastKing cDNA First Chain Synthesis Kit (TIANGEN, Beijing). The mRNA expression levels of *LRP1B*, *DNMT1*, *DNMT3A* and *DNMT3B* were determined by SYBR Green qPCR super mix (Invitrogen). *GAPDH* was selected as reference gene and the  $2^{-\Delta\Delta CT}$  method was used to analyze the difference of gene transcription level. The primer sequences of related genes are shown in Table 2.

### Western blot

The Pheo tissues or cells were treated with RIPA lysis buffer (Sigma-Aldrich) to obtain the total protein. The total protein was separated by sodium dodecyl sulfate-polyacrylamide gel electrophoresis (SDS-PAGE) and then transferred to polyvinylidene fluoride membrane (Millipore, MA, USA). After the transferred membrane was sealed with 5% skim milk, it was incubated with primary antibody at 4°C overnight. Then, the membrane was incubated with goat anti-rabbit IgG (1: 2000; Ab205718, Abcam) at room temperature for 2 h. Finally, the protein banding reaction was carried out by Western chemiluminescence HRP substrate (Abcam). Primary antibodies: *DNMT3A* (1:1000, ab307503, Abcam), *DNMT1* (1:1000, ab188453, Abcam), *DNMT3B* (1:1000, ab2851, Abcam), *LRP1B* (1: 2000, # PA5-115522, Thermo Fisher Scientific) and  $\beta$ -actin (1: 2000, ab8226, Abcam). Secondary antibodies: Rabbit Anti-Mouse IgG H&L (HRP) (1:2000, ab6728, Abcam).

### Methylation specific PCR (MSP)

The whole genome DNA of PC12 cells, cancer tissues and adjacent tissues were extracted, and then the DNA was modified and transformed by bisulfite by the EZ-DNA Methylation-Gold Kit (Zymo Research). The PCR primers of *LRP1B* promoter region were designed and synthesized to amplify the gDNA fragment transformed

**Table 3** MSP PCR primer sequence

Gene name	Forward primer	Reverse primer
LRP1B-MSP-M	TTTTTCGGGAAGGAAGTTTTTC	CATTAACCTAAAC-CAACCAAACG
LRP1B-MSP-U	TTTTTTTTGGGAAGGAAGTTTTT	ATTAACCTAAAC-CAACCAAACACC
ACTB-MSP-M	GTCGAATCGGGTATTGTTTAGC	GTCGAATCGGG-TATTGTTTAGC
ACTB-MSP-U	GGGTTGAATTGGGTATTGTTTAGT	AAAAAAAATTTTA-ACATTAACACC

by bisulfite. Primers for methylated (M) and unmethylated (U) promoter regions of *LRP1B* gene were designed through the Methprimer online program website (<http://www.urogene.org/cgi-bin/methprimer/methprimer.cgi>). We screened the *GAPDH* gene without methylation modification as a negative control group. The unmethylated DNA was modified using methylase, and the C base of CG in the DNA was methylated as a positive control. The related primers were listed in Table 3.

### Analysis of double luciferase reporter gene

The promoter region (2000 bp) of *LRP1B* was inserted in the promoter-less pmirGLO-empty vector (Promega) to construct wild-type vector (WT-*LRP1B*). The complete sequence of multiple G mutations to C in the 1000–1500 bp sequence of the *LRP1B* promoter by Sangon Biotech. The mutation sequence inserted into pmirGLO vector to construct mutant vector (*MUT-LRP1B*). PC12 cells transfected with oe-NC or oe-*DNMT3B* were inoculated into 16-well plates. Then, WT-*LRP1B* or *MUT-LRP1B* and the control empty plasmid pmirGLO were co-transfected into the above cells. After 48 h' culture, luciferase activity was detected by double luciferase assay kit (Promega).

### Chromatin Immunoprecipitation (ChIP)

The PC12 cells to be detected were cross-linked with formaldehyde solution. The CHIP kit (26157, Thermo Fisher) was used for relevant treatment. In short, the genomic DNA of PC12 was extracted, and DNA fragments were obtained by mechanical ultrasonic wave or microbial nuclease (MNase) digestion. Then, the lysate was immunoprecipitated with anti-*DNMT3B* (ab2851, Abcam) or negative control IgG (ab172730, Abcam).

**Table 4** CHIP-qPCR primer sequence

Gene name	Forward primer	Reverse primer
<i>LRP1B</i>	CATTGGACTTGGCTGTGGC	TGCTATGGCTGGGAATCGC

The enrichment of DNMT3B protein of specific DNA fragment with *LRP1B* promoter was measured by PCR, the related primers were in Table 4. Input was used as the control homogenization IP product ( $\Delta$ CT). The negative antibody was used to enrich the IgG product, and Input was also used to homogenize the product ( $\Delta$ CT). Finally, the difference in the number of amplification cycles after homogenization between IP and IgG ( $\Delta\Delta$ CT) was calculated, and the enrichment fold was calculated by  $2^{-\Delta\Delta$ CT}.

#### Colony formation assay

Cells were plated into a 12-well plate (500 cells/well) and cultured at 37°C for one week. Then, it was fixed with paraformaldehyde and dyed with 0.5% crystal violet solution for 20 min. Finally, the number of colonies was counted.

#### Transwell assays

Migration experiment: PC12 cells ( $1 \times 10^5$ ) were cultured in serum-free medium and plated in the upper chamber of a 12-wells Transwell system (with a pore size of 0.4  $\mu$ m). The culture medium containing 10% FBS was added to the lower chamber. After 24 h of culture, the cells in the lower chamber were fixed with 4% paraformaldehyde and stained with 0.1% crystal violet solution. Finally, the stained cells were observed under an optical microscope and photographed. In the invasion experiment, the bottom of the upper chamber was coated with matrix glue (BD Biosciences, USA), and the other operation steps were consistent with the migration experiment.

#### In vivo experiment

10 male BALB/c nude mice (4 weeks) were purchased from Guangdong Medical Laboratory Animal Center (Foshan, China). PC12 cells stably transfected with oe-NC or oe-*LRP1B* were collected. After washing twice with PBS solution, the cells were resuspended in serum-free DMEM ( $1 \times 10^7$ /mL) and subcutaneously injected into the armpit of nude mice (0.2 mL). After 28 days, mice were killed by dislocation of spine and tumors were collected. Hematoxylin-eosin staining (H&E) was used to detect the pathological changes of the tumor. Metastatic nodules in the lung specimens were counted under a light microscope.

#### Statistical analysis

All experimental results were expressed as mean  $\pm$  standard deviation (SD). Graphpad 8.0 was used for statistical analysis. *t* test was used for statistical analysis between

**Table 5** Relationship between *LRP1B* expression and clinicopathological features of pheochromocytoma

Classification	Total (%)	<i>LRP1B</i> expression		P value
		Low expression	High expression	
<b>Age</b>				0.552
<60	7	4	3	
$\geq$ 60	27	17	10	
<b>Sex</b>				0.406
Female	18	13	5	
Male	16	10	6	
<b>Tumor size (cm)</b>				0.110
<5 cm	14	6	8	
$\geq$ 5 cm	20	14	6	
<b>TNM stage</b>				0.068
I	13	10	3	
II	17	12	5	
III	4	3	1	
<b>Ki67 proliferation index</b>				0.012
<2	13	4	9	
$\geq$ 2	21	16	5	

the two groups, and one-way analysis of variance and Tukey's multiple comparison test were used for comparisons between groups.  $\chi^2$ -test was applied to analyze the correlations between *LRP1B* expression and clinicopathological characterization of Pheo patients. *P* value < 0.05 indicates significant difference.

## Results

### *LRP1B* was lowly-expressed in Pheo

To evaluate the expression level of *LRP1B* in Pheo tissues, we collected the samples derived from clinical interventions of 34 patients with Pheo at the early stage, and the clinical information was shown in Table 5. We showed that both the mRNA and protein levels of *LRP1B* were decreased in Pheo (Fig. 1A and B, *P* < 0.05). Moreover, the difference of *LRP1B* expression was related to Ki67 proliferation index of patients (Table 5). Consistently, IHC suggested that compared with the tissues adjacent to cancer, *LRP1B* was lowly expressed in Pheo, while Ki67 protein, a proliferation marker, was high expressed in Pheo (Fig. 1C, *P* < 0.05).

### *LRP1B* promoter was hypermethylated in Pheo

In line with the results from patient samples, the mRNA and protein levels of *LRP1B* were also reduced in Pheo cell line PC12 (Fig. 2A and B, *P* < 0.05). Since it has been already reported that *LRP1B* could be regulated at epigenetic level [9], we reasoned that the inhibited expression of *LRP1B* in Pheo cells might be related to an altered DNA methylation of *LRP1B* promoter in Pheo. Methprimer predicted that there were two CpG islands in the promoter region of *LRP1B* (Fig. 2C), which could be

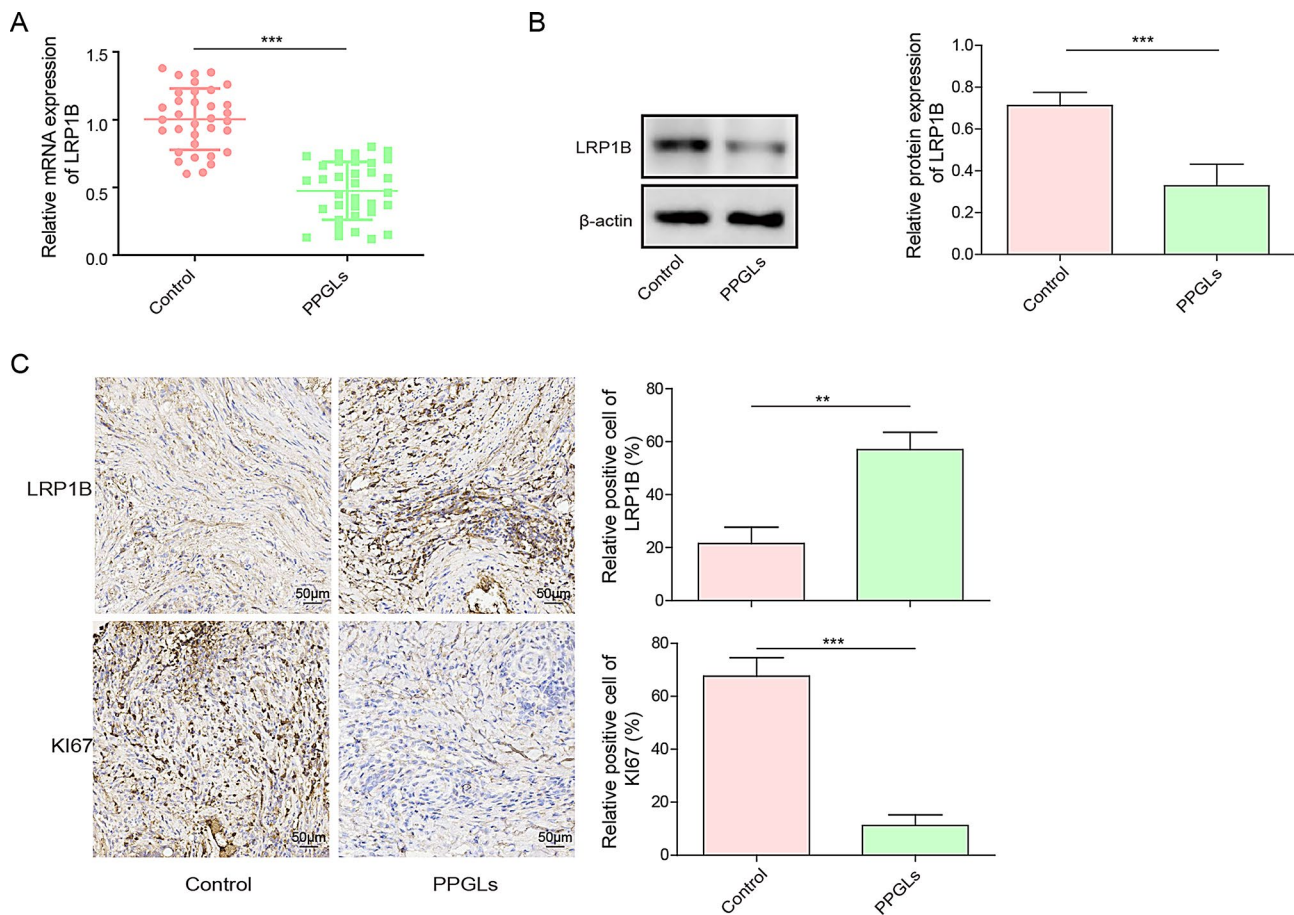


**Fig. 1** *LRP1B* was lowly-expressed in pheochromocytoma. **(A)** RT-qPCR showing the expression of *LRP1B* in Pheo and adjacent tissues. **(B)** Western blot showing the expression of *LRP1B* in Pheo and adjacent tissues **(C)** IHC showing the protein levels of *LRP1B* and *Ki67* in Pheo and adjacent tissues. All results were analyzed by t test. n=34, \* $P < 0.05$ , \*\* $P < 0.01$ , \*\*\* $P < 0.001$ . PPGLs: Pheochromocytomas and paragangliomas.

the potential methylated sites in Pheo cells. As expected, MSP assay showed that there was a high DNA methylation level in PC12 (Fig. 2D). Interestingly, we further analyzed the methylation level of *LRP1B* in cancer tissues and adjacent tissues of Pheo patients, and the results showed that *LRP1B* in cancer tissues had high methylation level (Fig. 2E). Considering the above observations, we hypothesized that the down-regulation of *LRP1B* in Pheo could result from the hypermethylation of *LRP1B* promoter.

#### DNMT3B could mediate the methylation of *LRP1B* promoter in Pheo

DNMT1, DNMT3A and DNMT3B are the predominate writers for DNA methylation [11]. To identify the writer catalyzing DNA methylation of *LRP1B* in Pheo, we first measured the expression levels of all three writers in Pheo tissues. While DNMT1 was similarly expressed by Pheo and cancer adjacent tissues, DNMT3A and DNMT3B were up-regulated in Pheo (Fig. 3A,  $P < 0.05$ ). Compared with DNMT3A, DNMT3B was more significantly up-regulated in Pheo (Fig. 3A,  $P < 0.05$ ). Moreover,

after knocking down *DNMT1*, *DNMT3A* or *DNMT3B* in PC12 cells, we found that *LRP1B* was up-regulated most significantly after knocking down *DNMT3B* (Fig. 3B,  $P < 0.05$ ). Therefore, we knocked down *DNMT3B* in PC12 cells using *DNMT3B* shRNAs. We observed that methylation of *LRP1B* promoter was decreased in the PC12 transfected with *DNMT3B* shRNAs (Fig. 3C,  $P < 0.05$ ). The direct interaction between DNMT3B and *LRP1B* promoter was further confirmed by luciferase assay and ChIP (Fig. 3E and F,  $P < 0.05$ ). The above results indicated that the methyltransferase DNMT3B inhibited *LRP1B* by mediating the methylation of *LRP1B* promoter in Pheo.

#### DNMT3B promoted the proliferation, migration and invasion of Pheo

To reveal how DNMT3B regulated the progression of Pheo, we identified cell proliferation, migration, and invasion of PC12 transfected with *DNMT3B* shRNAs. *DNMT3B* was efficiently silenced by all shRNAs, among which sh-*DNMT3B*-2 showed the highest efficiency (Fig. 4A and B,  $P < 0.05$ ). More important, when PC12 was transfected with sh-*DNMT3B*-2, cell proliferation,

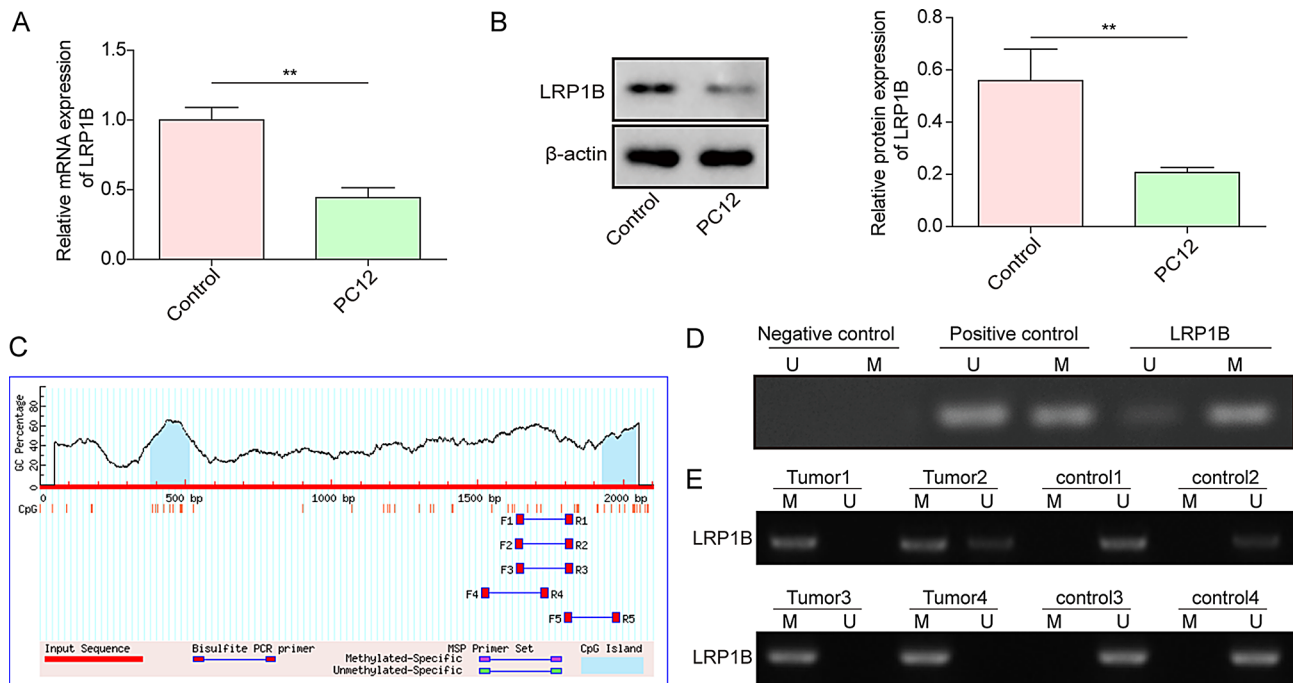


**Fig. 2** The promoter of *LRP1B* was hypermethylated in pheochromocytoma. **(A)** RT-qPCR showing the mRNA level of *LRP1B* in adrenal medullary cells and pheochromocytoma cells (PC12),  $n=34$ . **(B)** Western blot showing the expression of *LRP1B* in cells. **(C)** Methprimer showing the predicted CpG islands in the promoter region of *LRP1B*; **(D)** MSP showing the methylation of *LRP1B* in pheochromocytoma cells.  $n=3$ . **(E)** MSP showing the methylation of *LRP1B* in Pheo and adjacent tissues. All results were analyzed by t test.  $n=4$ \* $P<0.05$ , \*\* $P<0.01$ , \*\*\* $P<0.001$ .

migration, and invasion were significantly inhibited (Fig. 4D and E,  $P<0.05$ ). Therefore, *DNMT3B* promoted Pheo progression by enhancing the proliferation, migration, and invasion of tumor cells.

#### **DNMT3B promoted Pheo progression by repressing *LRP1B***

Since we have revealed the potential regulatory correlation between *DNMT3B* and *LRP1B* in Pheo, next we utilized rescue experiment to demonstrate that *DNMT3B* promoted Pheo by repressing the tumor repressive gene *LRP1B*. We simultaneously transfected PC12 with *DNMT3B* and (or) *LRP1B* overexpression vectors. The overexpression of *LRP1B* alone did not change the mRNA or protein of *DNMT3B*, whereas overexpression of *DNMT3B* alone reduced *LRP1B* protein levels. Co-overexpression of *DNMT3B* and *LRP1B* reversed the inhibitory effect of *DNMT3B* overexpression alone on *LRP1B* (Fig. 5A and B,  $P<0.05$ ). However, the overexpression of *DNMT3B* inhibited the exogenous expression of *LRP1B* in PC12 transfected with both oe-*DNMT3B* and oe-*LRP1B* (Fig. 5A and B). We also confirmed that the overexpression of *LRP1B* repressed the proliferation, migration and invasion of Pheo cells, which was compromised by *DNMT3B* overexpression (Fig. 5C and D,  $P<0.05$ ). The above results indicated that *DNMT3B* could promote Pheo progression by repressing *LRP1B*.

#### **Overexpression of *LRP1B* inhibited Pheo tumor growth in vivo**

Finally, we verified the repressive effect of *LRP1B* on Pheo in vivo using mouse model. In vivo transplantation showed that the Pheo tumor overexpressing *LRP1B* was apparently smaller than the control tumor (Fig. 6A and B,  $P<0.05$ ), suggesting the tumor suppressive role of *LRP1B*. H&E staining showed that tumor growth was inhibited in *LRP1B*-OE group (Fig. 6C,  $P<0.05$ ). Moreover, *LRP1B* inhibited the proliferation marker Ki67 in mice Pheo transplanted tumor (Fig. 6D,  $P<0.05$ ), further supporting that *LRP1B* inhibited Pheo.

#### **Discussion**

Due to the heterogeneity feature of Pheo, it's challenging to diagnose or treat this kind of neuroendocrine tumor [12]. Therefore, understanding the molecular mechanisms regulating tumor progression could shed new light on the diagnosis and treatments for Pheo [13]. In this study, we screened out *LRP1B* with significant differences in Pheo through TCGA database. It was revealed that the hypermethylation of the tumor suppressive gene *LRP1B* promoter, which was catalyzed by *DNMT3B*, was a potential cause of tumor progression and metastasis of Pheo.

*LRP1B* has been demonstrated to be a tumor suppressor gene [14] in several types of cancer. For instances, *LRP1B* had potential impacts on the efficacy of the

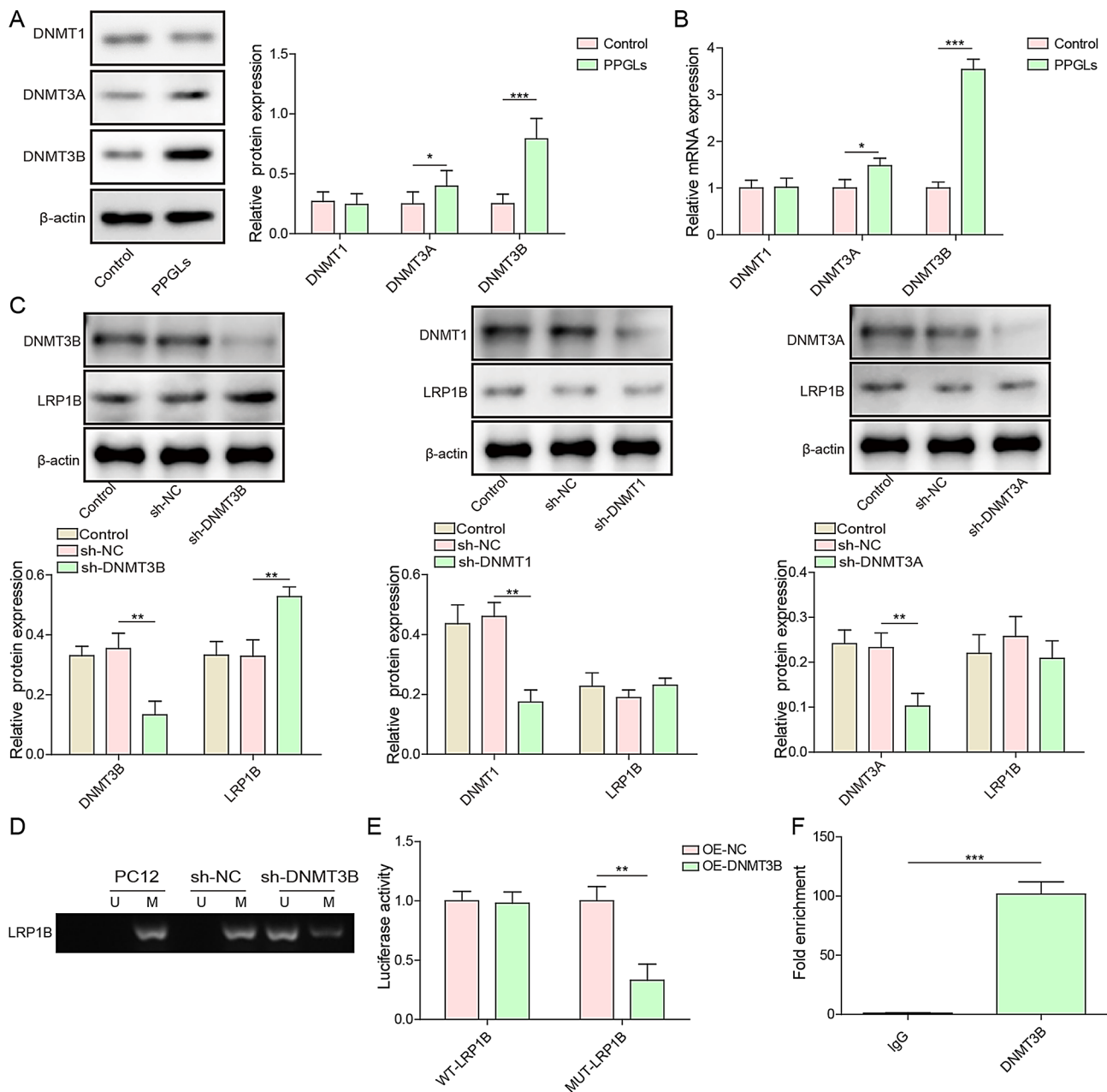


**Fig. 3** DNMT3B could directly bind to the promoter region of *LRP1B*. **(A)** RT-qPCR showing the expression levels of DNMT1, DNMT3A, and DNMT3B in pheochromocytoma. **(B)** RT-qPCR showing the expression of DNMT1, DNMT3A, and DNMT3B in PC12 cells. **(C)** Western blot was used to detect the changes of LRP1B protein expression after knocking down DNMT3A, DNMT3B or DNMT1, respectively. **(D)** MSP showing the methylation of LRP1B promoter was mediated by DNMT3B. **(E)** The interaction between DNMT3B and LRP1B promoter region was detected by dual luciferase reporter gene assay. **(F)** ChIP showing the interaction between DNMT3B and LRP1B promoter region. All results were analyzed by t test.  $n=3$ , \* $P<0.05$ , \*\* $P<0.01$ , \*\*\* $P<0.001$ .

immunotherapy for non-small cell lung cancer (NSCLC) [15]. The mutation of *LRP1B* was highly correlated with the incidence of ovarian cancer [16]. The copy number of *LRP1B* has found to be lost in thyroid carcinoma [17]. And to complement previous studies, here we reported that the abnormal epigenetic regulation of *LRP1B* was a driver of Pheo. We demonstrated that compared with adjacent noncancerous tissue, *LRP1B* had a lower expression level in Pheo. And our in vivo and in vitro

experiments suggested the tumor suppressive role of *LRP1B* in Pheo, as evidenced by the repressed proliferation, migration and invasion presented by *LRP1B*-overexpressed Pheo cells. It can be seen that *LRP1B* is also involved in regulating the progress of Pheo. Interestingly, our study found that low levels of *LRP1B* could increase the migration and invasion ability of PC12 cells. Metastatic pheochromocytoma and paraganglioma are usually difficult to treat and resistant to most conventional

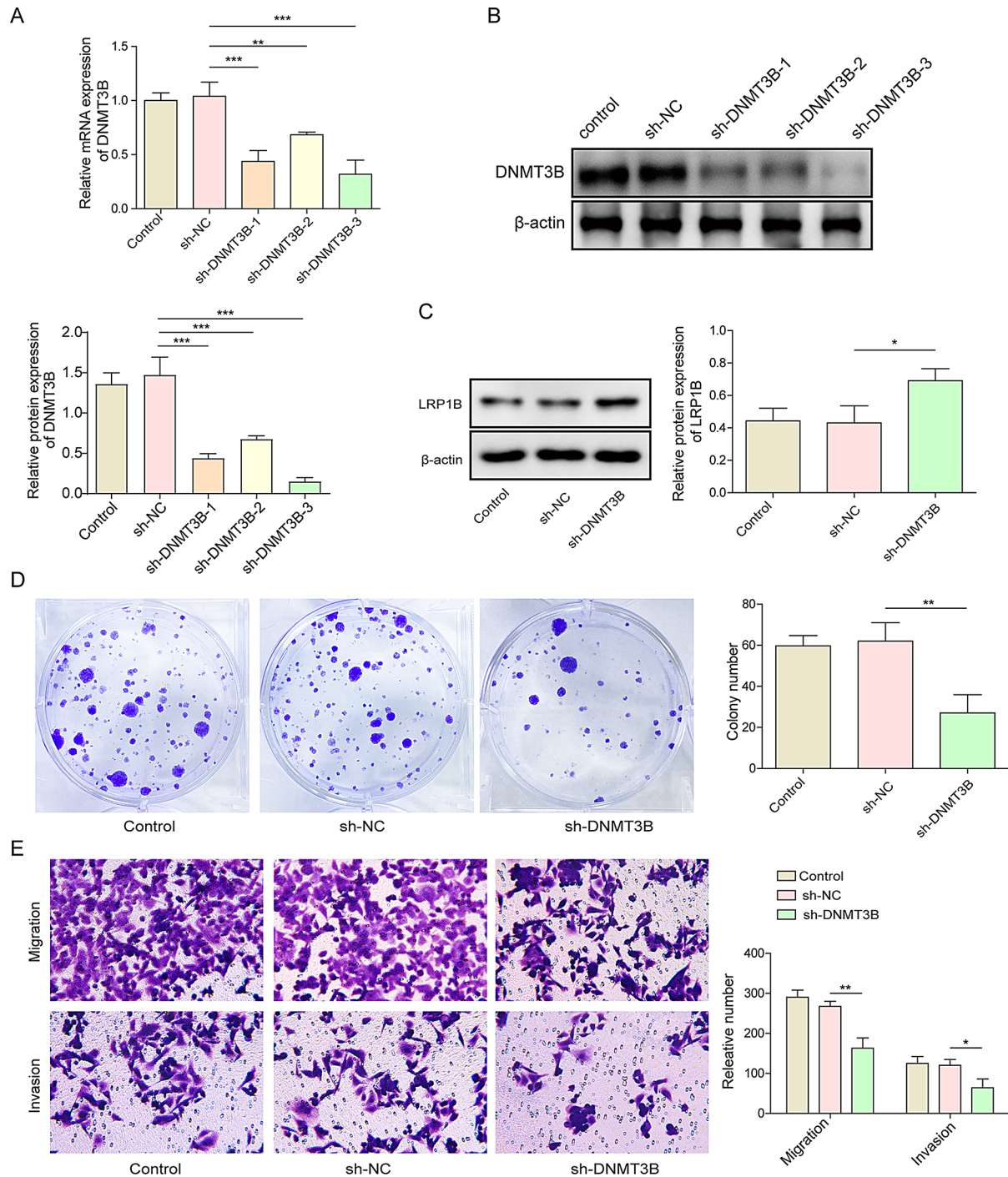


**Fig. 4** DNMT3B promoted the proliferation, migration and invasion of pheochromocytoma cells. **(A-B)** RT-qPCR and western blot showing the knock-down efficiency of sh-DNMT3B in PC12 cells. **(C)** Western blot showing LRP1B protein in PC12 cells. **(D)** Clonal formation showing the proliferation of PC12 cells. **(E)** Transwell showing the migration and invasion of PC12 cells. All results were analyzed by one-way ANOVA and Tukey multiple comparison test.  $n=3$ ,  $*P<0.05$ ,  $**P<0.01$ ,  $***P<0.001$

therapies [18]. Whether this regulatory role of LRP1B is also present in highly invasive murine Pheo MTT cells is worthy of investigation.

Using Methprimer, we predicted that within the promoter region of *LRP1B*, there were two CpG islands,

which were preferred by DNA methylation [19]. Further screening revealed that the methyltransferase responsible for the hypermethylation of *LRP1B* promoter in Pheo was DNMT3B, which has been widely studied in the progression of thyroid cancer, renal cancer, colorectal

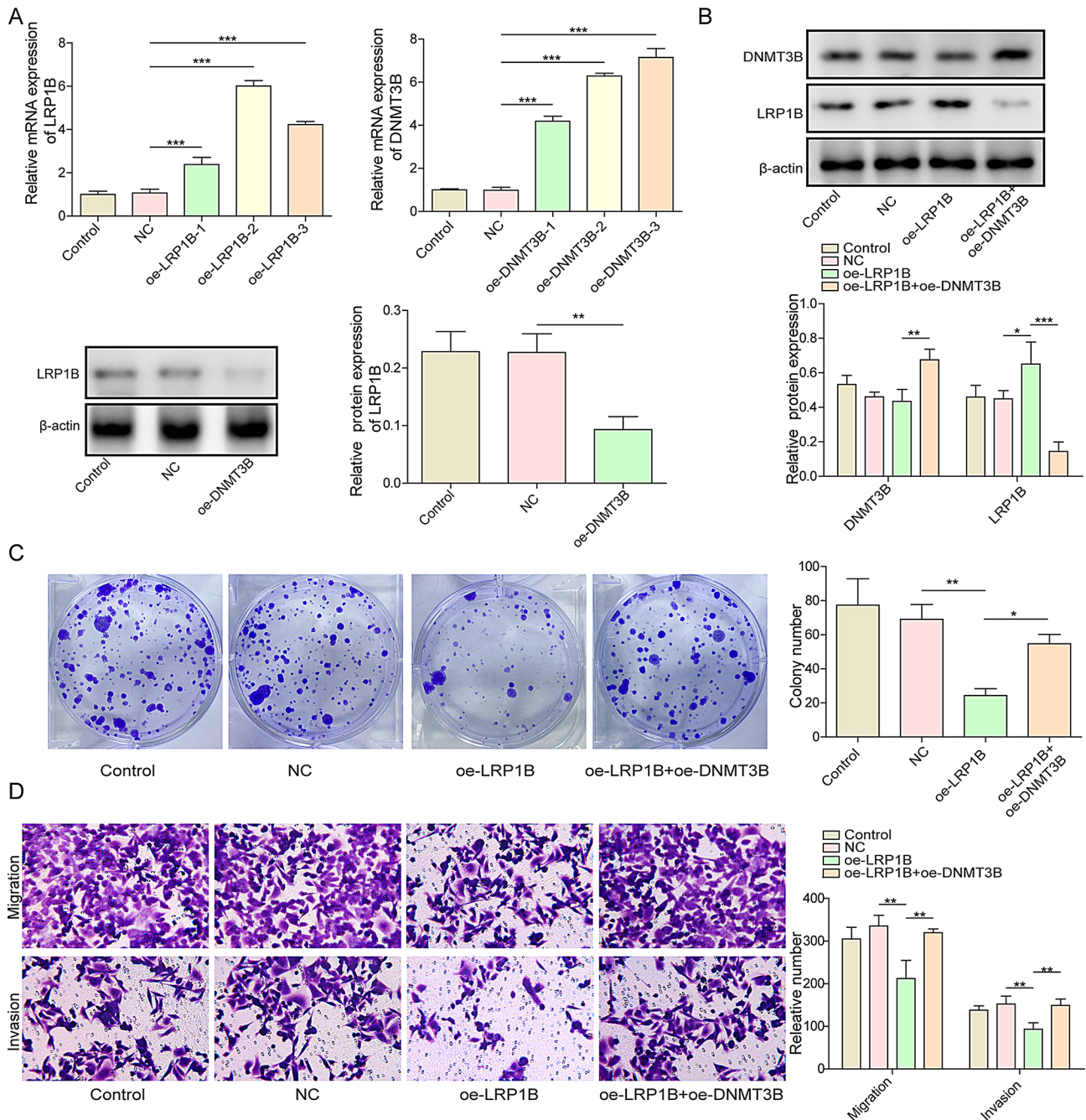


**Fig. 5** DNMT3B promoted the proliferation, migration and invasion of pheochromocytoma cells by regulating *LRP1B*. **(A)** RT-qPCR showing the mRNA levels of *DNMT3B* and *LRP1B* in PC12 cells. **(B)** Western blot showing the protein levels of DNMT3B and LRP1B. **(C)** Clonal formation showing the proliferation of PC12 cells. **(D)** Transwell showing the migration and invasion of PC12 cells. All results were analyzed by *one-way ANOVA* and *Tukey multiple comparison test*.  $n=3$ ,  $*P<0.05$ ,  $**P<0.01$ ,  $***P<0.001$

cancer, and other tumors [25–27]. We observed a reversed expression pattern of *LRP1B* and *DNMT3B* in the clinical samples as well as the cell line PC12 of Pheo. Specifically, *LRP1B* was lowly expressed while *DNMT3B* was highly expressed in Pheo. Leveraging biochemistry assays including luciferase and ChIP, we demonstrated the direct interaction between DNMT3B and *LRP1B*

promoter. More importantly, our functional assays, especially the rescue experiment, suggested the progression of Pheo was regulated by the *DNMT3B-LRP1B* axis.

In recent years, besides the tumor cells themselves, the stromal cells and immune cells of Pheo are also of great significance for understanding tumor biology and treatment [23]. At present, our research on Pheo is

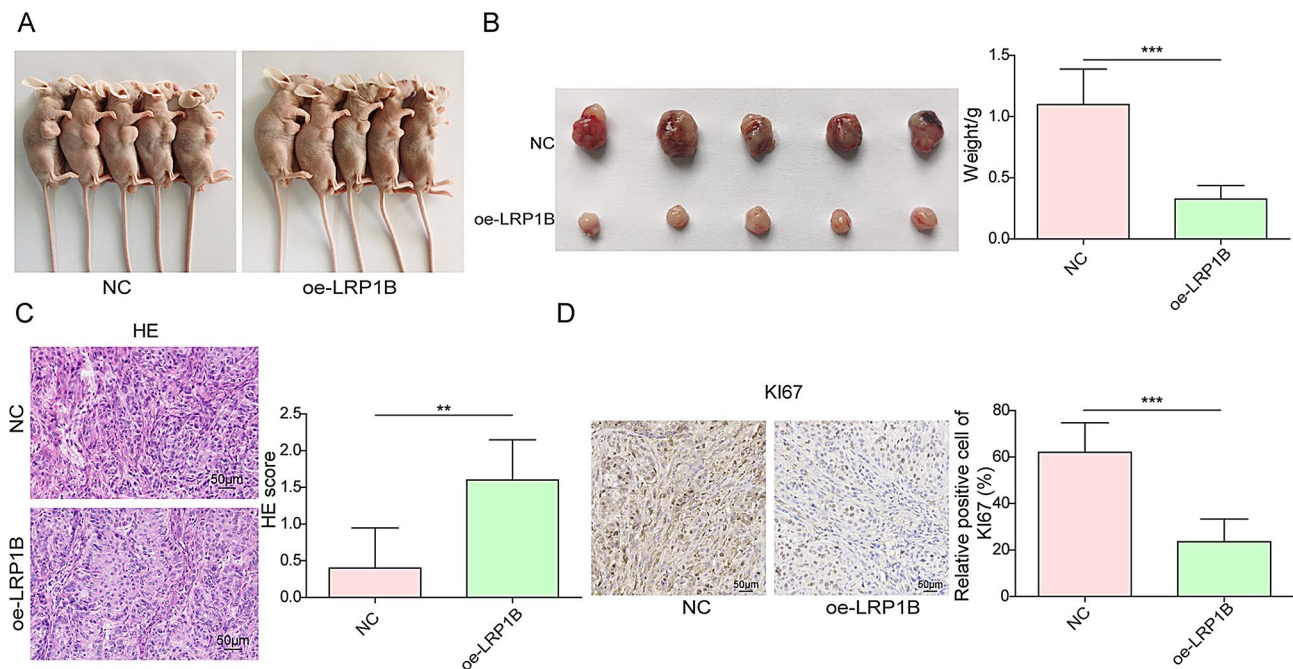


**Fig. 6** *LRP1B* inhibits tumor growth of pheochromocytoma in vivo. Transplanted tumor was formed by transfection of OE-NC or OE-*LRP1B* into Pheo cells, followed by subcutaneous injection into mice. **(A)** Image showing the tumor engraftments. **(B)** Isolation and display diagram of mouse tumor. **(C)** H&E staining of the tumor engraftments. **(D)** IHC showing the expression of Ki67 in transplanted tumor of mice in each group. All results were analyzed by t test.  $n=5$ , \* $P<0.05$ , \*\* $P<0.01$ , \*\*\* $P<0.001$ .

mainly concentrated in Pheo cells, and the regulation of *DNMT3B-LRP1B* axis is also mainly in Pheo cells. It was found that the expression of *LRP1B* in gastric cancer was related to the infiltration of  $CD4^+$  T cells and macrophages [24]. *DNMT3B* can regulate tumor microenvironment and affect cancer chemotherapy sensitivity [25]. Recent studies have found that some cell types (including fibroblasts and macrophages) in tumor microenvironment can also regulate the characteristics of Pheo cells [26], [27]. Therefore, our research can continue to explore whether the *DNMT3B-LRP1B* axis affects other cells in the Pheo microenvironment.

It's noteworthy that the dysregulation of *LRP1B* in a variety of tumor cells has been attributed to the abnormal epigenetic modification, including DNA methylation and histone acetylation [28]. In esophageal carcinoma, *LRP1B* loss-of-function mutation is related to transcriptional silencing caused by hypermethylation of CpG island [29]. DNA copy number loss and CpG island methylation of *LRP1B*, which inhibit *LRP1B* gene expression, are frequently present in cancer tissues, which led to low mRNA expression [30–32]. Here we have only identified one potential epigenetic modification contributing to the repression of *LRP1B* in Pheo. Whether other epigenetic modifications, such as histone modifications and even RNA methylations, were also involved in regulating *LRP1B* in Pheo is worth to be studied in the future. Taken together, our study has improved the understanding

towards Pheo progression by firstly reporting an epigenetic regulatory mechanism controlling the proliferation, migration, and invasion of Pheo tumor cells. And this study would provide new insights into the diagnosis and treatments for Pheo.

### Supplementary Information

The online version contains supplementary material available at <https://doi.org/10.1186/s13072-025-00592-8>.

Supplementary Material 1

Supplementary Material 2

### Acknowledgements

Not applicable.

### Author contributions

Conceptualization: Min Sun, Jiuzhi Li. Methodology: Jing Wan, Bingli Zheng. Software: Zhenfeng Shi, Jiuzhi Li. Validation: Zhenfeng Shi, Yanrong Ma. Formal analysis: Jing Wan, Bingli Zheng. Investigation: Min Sun, Zhenfeng Shi, Jiuzhi Li. Resources: Min Sun, Yanrong Ma. Data Curation: Jing Wan, Bingli Zheng. Writing - Original Draft: Min Sun. Writing - Review & Editing: Zhenfeng Shi, Yanrong Ma. Visualization: Yanrong Ma, Jiuzhi Li. Supervision: Min Sun. Project administration: Min Sun. All authors read and approved the final manuscript.

### Funding

This study was supported by Xinjiang Natural Science Foundation General Project (Grant No. 2022D01C630), National Natural Science Foundation of China Regional Project (Grant No. 82360520), Xinjiang Natural Science Foundation for Distinguished Young Scholars (Grant No. 2022D01E84) and Xinjiang Tianshan Talent Training Program (Grant No. 2023TSYCCX0061).

### Data availability

All data generated or analysed during this study are included in this article.

### Declarations

### Ethical approval

The collection of tissue samples obtained approval from the Ethics Committee of People's Hospital of Xinjiang Uygur Autonomous Region (No. KY2023060156).

### Competing interests

The authors declare no competing interests.

Received: 29 October 2024 / Accepted: 23 April 2025

Published online: 09 May 2025

### References

1. Calsina B, Piñeiro-Yáñez E, Martínez-Montes AM, Caleiras E, Fernández-Sanromán A, Monteagudo M, Torres-Pérez R, Fustero-Torre C, Pulgarín-Alfaro M, Gil E et al. Genomic and immune landscape of metastatic pheochromocytoma and paraganglioma. *Nat Commun.* 2023;14(1). <https://doi.org/10.1038/s41467-023-36769-6>. PMID: WOS:000955827800007. ARTN 1122.
2. Carrasquillo JA, Chen CC, Jha A, Ling A, Lin F, Pryma DA, Pacak K. Imaging of pheochromocytoma and paraganglioma. *J Nucl Med.* 2021;62(8):1033–42. <https://doi.org/10.2967/jnumed.120.259689>. PMID: WOS:000711570000009.
3. Martinelli S, Amore F, Canu L, Maggi M, Rapizzi E. Tumour microenvironment in pheochromocytoma and paraganglioma. *Front Endocrinol.* 2023;14. <https://doi.org/10.3389/fendo.2023.1137456>. PMID: WOS:000963005200001. ARTN 1137456.
4. Lima JV, Kater CE. The pheochromocytoma/paraganglioma syndrome: an overview on mechanisms, diagnosis and management. *Int Braz J Urol.* 2023;49(3):307–19. <https://doi.org/10.1590/S1677-5538.Ibju.2023.0038>. PMID: WOS:001021771100004.
5. Ye C, Chong W, Liu Y, Zhu X, Ren H, Xu K, Xie X, Du F, Zhang Z, Wang M, et al. Suppression of tumorigenesis in LUAD by LRP1B through regulation of the IL-6-JAK-STAT3 pathway. *Am J Cancer Res.* 2023;13(7):2886–905. PMID: 37560001.
6. Brown LC, Tucker MD, Sedhom R, Schwartz EB, Zhu J, Kao C, Labriola MK, Gupta RT, Marin D, Wu Y, et al. LRP1B mutations are associated with favorable outcomes to immune checkpoint inhibitors across multiple cancer types. *J Immunother Cancer.* 2021;9(3). <https://doi.org/10.1136/jitc-2020-001792>. PMID: 33653800.
7. Wang Z, Sun P, Gao C, Chen J, Li J, Chen Z, Xu M, Shao J, Zhang Y, Xie J. Down-regulation of LRP1B in colon cancer promoted the growth and migration of cancer cells. *Exp Cell Res.* 2017;357(1):1–8. <https://doi.org/10.1016/j.yexcr.2017.04.010>. PMID: 28408316.
8. Asano Y, Takeuchi T, Okubo H, Saigo C, Kito Y, Iwata Y, Futamura M, Yoshida K. Nuclear localization of LDL receptor-related protein 1B in mammary gland carcinogenesis. *J Mol Med (Berl).* 2019;97(2):257–68. <https://doi.org/10.1007/s00109-018-01732-2>. PMID: 30607440.
9. Príncipe C, de Sousa IJD, Prazeres H, Soares P, Lima RT. LRP1B: A giant lost in Cancer translation. *Pharmaceuticals-Base.* 2021;14(9). <https://doi.org/10.3390/ph14090836>. PMID: WOS:000701275400001. ARTN 836.
10. Ohshima Y, Sudo H, Watanabe S, Nagatsu K, Tsuji AB, Sakashita T, Ito YM, Yoshinaga K, Higashi T, Ishioka NS. Antitumor effects of radionuclide treatment using alpha-emitting meta-(211)At-astato-benzylguanidine in a PC12 pheochromocytoma model. *Eur J Nucl Med Mol Imaging.* 2018;45(6):999–1010. <https://doi.org/10.1007/s00259-017-3919-6>. PMID: 29350258.
11. Li JS, Su XL, Dai L, Chen N, Fang C, Dong ZX, Fu JM, Yu Y, Wang WS, Zhang HT, et al. Temporal DNA methylation pattern and targeted therapy in colitis-associated cancer. *Carcinogenesis.* 2020;41(2):235–44. <https://doi.org/10.1093/carcin/bgz199>. PMID: WOS:000537366000012.
12. Leung K, Stamm M, Raja A, Low G. Pheochromocytoma. The range of appearances on ultrasound, CT, MRI, and functional imaging. *Am J Roentgenol.* 2013;200(2):370–8. <https://doi.org/10.2214/Ajr.12.9126> PMID: WOS:000313957400037.
13. Ullrich M, Richter S, Liers J, Drukewitz S, Friedemann M, Kotzerke J, Ziegler CG, Nölting S, Kopka K, Pietzsch J. Epigenetic drugs in somatostatin type 2 receptor radionuclide theranostics and radiation transcriptomics in mouse pheochromocytoma models. *Theranostics.* 2023;13(1):278–94. <https://doi.org/10.7150/thno.77918>. PMID: WOS:000894576600003.
14. Rui Wang GZ, Zhu X, Xu Y, Cao N, Li Z, Han C, Shen MQY, Dong J, Zhao FMA. Prognostic Implications of LRP1B and Its Relationship with the Tumor-Infiltrating Immune Cells in Gastric Cancer. *Cancers.* 2023;15(24):5759. <https://doi.org/10.3390/cancers15245759>
15. Hao F, Ma Q, Zhong DS. Potential predictive value of comutant LRP1B and FAT for immune response in non-small cell lung cancer LRP1B and FAT comutation enhance immune response. *Transl Oncol.* 2022;24. <https://doi.org/10.1016/j.tranon.2022.101493> PMID: WOS:000835517900004. ARTN 101493.
16. de Sousa IJD, Cunha AI, Saraiva IA, Portugal RV, Gimba ERP, Guimaraes M, Prazeres H, Lopes JM, Soares P, Lima RT. LRP1B expression as a putative predictor of response to pegylated liposomal doxorubicin treatment in ovarian Cancer. *Pathobiology.* 2021;88(6):400–11. <https://doi.org/10.1159/000517372> PMID: WOS:000713908500001.
17. Prazeres H, Torres J, Rodrigues F, Pinto M, Pastoriza MC, Gomes D, Cameselle-Teijeiro J, Vidal A, Martins TC, Sobrinho-Simoes M, et al. Chromosomal, epigenetic and microRNA-mediated inactivation of LRP1B, a modulator of the extracellular environment of thyroid cancer cells (30, Pg 1302, 2010). *Oncogene.* 2017;36(1):146. <https://doi.org/10.1038/ncr.2016.143>. PMID: WOS:000394069100013.
18. Nolting S, Giubellino A, Tayem Y, Young K, Lauseker M, Bullova P, Schovaneck J, Anver M, Fliedner S, Korbonits M, et al. Combination of 13-Cis retinoic acid and Lovastatin: marked antitumor potential in vivo in a pheochromocytoma allograft model in female athymic nude mice. *Endocrinology.* 2014;155(7):2377–90. <https://doi.org/10.1210/en.2014-1027> PMID: 24762141. 10.1210/en.2014-1027.
19. Sergeeva A, Davydova K, Perenkov A, Vedunova M. Mechanisms of human DNA methylation, alteration of methylation patterns in physiological processes and oncology. *Gene.* 2023;875. <https://doi.org/10.1016/j.gene.2023.147487>. PMID: WOS:001011456200001. ARTN 147487.
20. Zhu X, Xue CY, Kang XF, Jia XM, Wang L, Younis MH, Liu DH, Huo N, Han YC, Chen Z et al. DNMT3B-mediated FAM111B methylation promotes papillary thyroid tumor glycolysis, growth and metastasis. *Int J Biol Sci.* 2022;18(11):4372–87. <https://doi.org/10.7150/ijbs.72397>. PMID: WOS:000832879400008.
21. Quan Z, He YF, Luo CL, Xia Y, Zhao Y, Liu NJ, Wu XH. Interleukin 6 induces cell proliferation of clear cell renal cell carcinoma by suppressing Hepa-CAM via the STAT3-dependent up-regulation of DNMT1 or DNMT3B. *Cell Signal.* 2017;32:48–58. <https://doi.org/10.1016/j.cellsig.2017.01.017>. PMID: WOS:000395953400005.
22. Ren GL, Li HY, Hong D, Hu FY, Jin RJ, Wu S, Sun WH, Jin HL, Zhao LL, Zhang XD et al. LINC00955 suppresses colorectal cancer growth by acting as a molecular scaffold of TRIM25 and Sp1 to inhibit DNMT3B-mediated methylation of the PHIP promoter. *BMC Cancer.* 2023;23(1). <https://doi.org/10.1186/s12885-023-11403-2>. PMID: WOS:001075729700003. ARTN 898.
23. Zethoven M, Martelotto L, Pattison A, Bowen B, Balachander S, Flynn A, Rosello FJ, Hogg A, Miller JA, Fryszak Z, et al. Single-nuclei and bulk-tissue gene-expression analysis of pheochromocytoma and paraganglioma links disease subtypes with tumor microenvironment. *Nat Commun.* 2022;13(1):6262. <https://doi.org/10.1038/s41467-022-34011-3>. PMID: 36271074.
24. Wang R, Zhang G, Zhu X, Xu Y, Cao N, Li Z, Han C, Qin M, Shen Y, Dong J, et al. Prognostic implications of LRP1B and its relationship with the Tumor-Infiltrating immune cells in gastric Cancer. *Cancers (Basel).* 2023;15(24). <https://doi.org/10.3390/cancers15245759>. PMID: 38136305.
25. Song Y, Kim N, Heo J, Shum D, Heo T, Seo HR. Inhibition of DNMT3B expression in activated hepatic stellate cells overcomes chemoresistance in the tumor microenvironment of hepatocellular carcinoma. *Sci Rep.* 2024;14(1):115. <https://doi.org/10.1038/s41598-023-50680-6>. PMID: 38168140.
26. Martinelli S, Rivero M, Mello T, Amore F, Parri M, Simeone I, Mannelli M, Maggi M, Rapizzi E. SDHB and SDHD silenced pheochromocytoma spheroids respond differently to tumour microenvironment and their aggressiveness is inhibited by impairing stroma metabolism. *Mol Cell Endocrinol.* 2022;547:111594. <https://doi.org/10.1016/j.mce.2022.111594>. PMID: 35149119.
27. Martinelli S, Amore F, Canu L, Maggi M, Rapizzi E. Tumour microenvironment in pheochromocytoma and paraganglioma. *Front Endocrinol (Lausanne).* 2023;14:1137456. <https://doi.org/10.3389/fendo.2023.1137456>. PMID: 37033265.
28. Ni SB, Hu JR, Duan YS, Shi SL, Li R, Wu HJ, Qu YP, Li Y. Down expression of promotes cell migration via RhoA/Cdc42 pathway and actin cytoskeleton

- remodeling in renal cell cancer. *Cancer Sci.* 2013;104(7):817–25. <https://doi.org/10.1111/cas.12157>. PMID: WOS:000325680000006.
29. Sonoda I, Imoto I, Inoue J, Shibata T, Shimada Y, Chin K, Imamura M, Amagasa T, Gray JW, Hirohashi S, et al. Frequent Silencing of low density lipoprotein receptor-related protein 1B (LRP1B) expression by genetic and epigenetic mechanisms in esophageal squamous cell carcinoma. *Cancer Res.* 2004;64(11):3741–7. <https://doi.org/10.1158/0008-5472.CAN-04-0172>. PMID: 15172977.
  30. Prazeres H, Torres J, Rodrigues F, Pinto M, Pastoriza MC, Gomes D, Cameselle-Teijeiro J, Vidal A, Martins TC, Sobrinho-Simoes M, et al. Chromosomal, epigenetic and microRNA-mediated inactivation of LRP1B, a modulator of the extracellular environment of thyroid cancer cells. *Oncogene.* 2011;30(11):1302–17. <https://doi.org/10.1038/onc.2010.512>. PMID: 21057533.
  31. Sadee W, Wang D, Hartmann K, Toland AE. Pharmacogenomics: driving personalized medicine. *Pharmacol Rev.* 2023;75(4):789–814. <https://doi.org/10.1124/pharmrev.122.000810>. PMID: 36927888.
  32. Li SY, Sun R, Wang HX, Shen S, Liu Y, Du XJ, Zhu YH, Jun W. Combination therapy with epigenetic-targeted and chemotherapeutic drugs delivered by nanoparticles to enhance the chemotherapy response and overcome resistance by breast cancer stem cells. *J Control Release.* 2015;205:7–14. <https://doi.org/10.1016/j.jconrel.2014.11.011>. PMID: 25445694.

### Publisher's note

Springer Nature remains neutral with regard to jurisdictional claims in published maps and institutional affiliations.